

THE 2-TORSION IN THE FARRELL–TATE COHOMOLOGY OF $\mathrm{PSL}_4(\mathbb{Z})$, AND TORSION SUBCOMPLEX REDUCTION VIA DISCRETE MORSE THEORY

ANH TUAN BUI^{1,2}, ALEXANDER D. RAHM³ AND MATTHIAS WENDT⁴

ABSTRACT. In the present paper, we use discrete Morse theory to provide a new implementation of torsion subcomplex reduction for arithmetic groups. This leads both to a simpler algorithm as well as runtime improvements. To demonstrate the technique, we compute the mod 2 Farrell–Tate cohomology of $\mathrm{PSL}_4(\mathbb{Z})$.

1. INTRODUCTION

In this paper, we compute the dimension of the mod 2 group cohomology $H^q(\mathrm{PSL}_4(\mathbb{Z}); \mathbb{F}_2)$ of the rank 4 projective special linear group $\mathrm{PSL}_4(\mathbb{Z})$ over the natural integers \mathbb{Z} , above the virtual cohomological dimension (vcd) of $\mathrm{PSL}_4(\mathbb{Z})$, which is 6 according to Borel and Serre’s formula [2]. We obtain the result, displayed in Theorem 1.1, via a computation of the associated Farrell–Tate cohomology, which (with prime coefficients) is isomorphic to group cohomology in degrees above the vcd.

Theorem 1.1. *The mod-2 Farrell–Tate cohomology of $\mathrm{PSL}_4(\mathbb{Z})$ has the following dimensions over \mathbb{F}_2 in degrees $0 \leq q \leq 6$:*

| q | 0 | 1 | 2 | 3 | 4 | 5 | 6 |
|---|---|---|---|---|---|----|----|
| $\dim_{\mathbb{F}_2} \widehat{H}^q(\mathrm{PSL}_4(\mathbb{Z}); \mathbb{F}_2)$ | 1 | 0 | 5 | 7 | 7 | 17 | 27 |

In degrees above $7 \leq q \leq 42$, the dimension of the Farrell–Tate cohomology $\dim_{\mathbb{F}_2} \widehat{H}^q(\mathrm{PSL}_4(\mathbb{Z}); \mathbb{F}_2)$ and hence the dimension of the group cohomology $\dim_{\mathbb{F}_2} H^q(\mathrm{PSL}_4(\mathbb{Z}); \mathbb{F}_2)$, equals the number $\dim_{\mathbb{F}_2} E_2^{0,q}$ computed in Table 1.

A contractible cell complex with a proper action of $\mathrm{PSL}_4(\mathbb{Z})$ was already available on computers in 2002 [9, 10], and one of the authors (A.R.) did pick up the task of computing the cohomology of $\mathrm{PSL}_4(\mathbb{Z})$ at small primes as his PhD thesis project in 2007, but in order to deal with prime numbers present in the orders of cell stabilizers, a whole new set of sophisticated tools had to be developed over the years, documented in a series of publications by the authors. The final tool was recently contributed by Ellis [11]. That is why the mod 2 cohomology of $\mathrm{PSL}_4(\mathbb{Z})$ has only been computed in the present paper, 47 years after the mod 2 cohomology computation for $\mathrm{SL}_3(\mathbb{Z})$ by Soulé [24].

In Sections 3 to 5, we detail our computations, and in Section 6, we point out their consequences on Steinberg homology.

Also in this paper, we provide a further tool, which can help other mathematicians to compute small prime cohomology of more complicated arithmetic groups. Namely, in Section 2, we modify discrete Morse theory to arrive at very small complexes of groups describing the E_1 -page of the equivariant spectral sequence for an arithmetic group. Our modification deals with the fact that we are not just interested in the cohomology of a cell complex, but actually the equivariant cohomology of a complex of groups. If we are interested specifically in Farrell–Tate or group cohomology at a single prime number ℓ , our discrete Morse theory method is an improvement over the previously used torsion subcomplex reduction methods. The modification of discrete Morse

Date: July 22, 2025.

2020 Mathematics Subject Classification. 11F75, Cohomology of arithmetic groups.

Key words and phrases. Projective special linear group of rank 4.

TABLE 1. The E_2 -page of the equivariant spectral sequence converging to the mod 2 Farrell–Tate cohomology of $\mathrm{PSL}_4(\mathbb{Z})$ is, in degrees $q \geq 2$, concentrated in the single column $p = 0$. In that column, we record the following dimensions over \mathbb{F}_2 for $E_2^{0,q}$ for $7 \leq q \leq 42$:

| | | | | | | | | | | | | | | | | | |
|---------------------------------|------|------|------|------|------|------|------|------|------|------|------|------|------|------|-----|-----|-----|
| q | 7 | 8 | 9 | 10 | 11 | 12 | 13 | 14 | 15 | 16 | 17 | 18 | 19 | 20 | 21 | 22 | 23 |
| $\dim_{\mathbb{F}_2} E_2^{0,q}$ | 31 | 50 | 67 | 78 | 107 | 134 | 153 | 195 | 233 | 263 | 319 | 371 | 413 | 486 | 553 | 610 | 701 |
| q | 24 | 25 | 26 | 27 | 28 | 29 | 30 | 31 | 32 | 33 | 34 | 35 | 36 | 37 | | | |
| $\dim_{\mathbb{F}_2} E_2^{0,q}$ | 786 | 859 | 971 | 1075 | 1167 | 1301 | 1427 | 1539 | 1698 | 1847 | 1982 | 2167 | 2342 | 2501 | | | |
| q | 38 | 39 | 40 | 41 | 42 | | | | | | | | | | | | |
| $\dim_{\mathbb{F}_2} E_2^{0,q}$ | 2715 | 2917 | 3103 | 3347 | 3579 | | | | | | | | | | | | |

theory we propose produces significantly smaller cell complexes and therefore simplifies the equivariant spectral sequence calculations. The Morse-theoretic torsion subcomplex reduction provides a description of the (mod ℓ) E_1 -page of the equivariant spectral sequence which yields again the original E_2 -page, hence the computations provide descriptions of Farrell–Tate cohomology in all degrees.

We do not aim at developing a very general equivariant version of discrete Morse theory, as this has already been done in the literature [14, 25]. Rather, we want to provide a specific tool for studying arithmetic groups at a single prime number ℓ , which is not provided in Yerolemou and Nanda’s approach, which requires the group under study to be finite [25], while Freij’s approach is not designed for the study at a single prime number [14].

The object which we shall reduce using Discrete Morse Theory, is the ℓ -torsion subcomplex at a prime number ℓ . In order to compute the mod ℓ Farrell–Tate cohomology of a group from its proper action on a contractible cell complex, it is enough to study the action on the ℓ -torsion subcomplex [22]. Our reduction of the latter brings further arithmetic groups within reach.

Definition 1.2. *For ℓ a prime number, the ℓ -torsion subcomplex is the set of all cells with stabilizers containing some element(s) of order ℓ .*

For the ℓ -torsion subcomplex to be guaranteed to be a cell complex, and to consist only of fixed points of order- ℓ -elements (so to coincide with the ℓ -singular part), we need a rigidity property: We want each cell stabilizer to fix its cell pointwise. In theory, it is always possible to obtain this rigidity property via the barycentric subdivision. In practice, to avoid a memory stack overflow, we need to use the cell subdivision algorithms “rigid facets subdivision” and “virtually simplicial subdivision” provided in previous work of the authors [6], because the barycentric subdivision of an n -dimensional cell complex can multiply the number of cells by $(n + 1)!$.

The rigid cell complexes returned by rigid facets subdivision are rather big, compared to the non-rigid complexes we start with (–for the full cell complex, see table 1 in the paper where the mod 3 Farrell–Tate cohomology of $\mathrm{PSL}_4(\mathbb{Z})$ was computed [6]; –for the 2-torsion subcomplex, we reprint Table 2 here from that paper with the kind permission of the authors;–). To reduce the size of the complexes (as well as the size of the resulting spectral sequences), we now discuss a variant of discrete Morse theory taking into account the additional information of stabilizer subgroups: the gradient flow is only allowed to proceed in directions where the cohomology of the stabilizer subgroups does not change, as specified in Condition 2.1 below. In our computation, the number of critical cells is significantly smaller than the number of cells before reduction, and the restriction on stabilizer subgroups implies that the E_1 -page produces again the original E_2 -page of the equivariant spectral sequence.

Structure of the paper. We first discuss how torsion subcomplex reduction can be realized by a version of discrete Morse theory taking into account fusion control for stabilizer subgroups in Section 2. The example of the reduced torsion subcomplex for $\mathrm{PSL}_4(\mathbb{Z})$ is discussed in Section 3. In Section 4, we assemble the d_1 differential of the equivariant spectral sequence, which was the

TABLE 2. Numbers of cells in the 2-torsion subcomplex for $\mathrm{PSL}_4(\mathbb{Z})$ before reduction, obtained after rigid facets subdivision of the studied cell complex, sorted into isomorphism types of their stabilizers. Here, G_1 and G_2 are non-trivial group extensions $1 \rightarrow \mathcal{A}_4 \times \mathcal{A}_4 \rightarrow G_1 \rightarrow \mathbb{Z}/2\mathbb{Z} \rightarrow 1$ and $1 \rightarrow G_0 \rightarrow G_2 \rightarrow \mathbb{Z}/2\mathbb{Z} \rightarrow 1$ for $1 \rightarrow (\mathbb{Z}/2\mathbb{Z})^4 \rightarrow G_0 \rightarrow \mathbb{Z}/3\mathbb{Z} \rightarrow 1$.

| Stabilizer type | \mathcal{A}_4 | G_1 | $(\mathbb{Z}/2\mathbb{Z})^2$ | S_4 | $\mathbb{Z}/2\mathbb{Z}$ | \mathcal{D}_8 | $(\mathbb{Z}/2\mathbb{Z})^3$ | G_2 | $\mathbb{Z}/4\mathbb{Z}$ |
|-----------------|-----------------|-------|------------------------------|-------|--------------------------|-----------------|------------------------------|-------|--------------------------|
| Vertices | 2 | 1 | 5 | 4 | 1 | 2 | 1 | 1 | 0 |
| Edges | 2 | 0 | 24 | 2 | 101 | 5 | 1 | 0 | 5 |
| 2-cells | 0 | 0 | 27 | 0 | 326 | 0 | 0 | 0 | 4 |
| 3-cells | 0 | 0 | 8 | 0 | 340 | 0 | 0 | 0 | 0 |
| 4-cells | 0 | 0 | 0 | 0 | 116 | 0 | 0 | 0 | 0 |

major technical task of this paper. The spectral sequence computations for the mod 2 Farrell–Tate cohomology of $\mathrm{PSL}_4(\mathbb{Z})$ are carried out in Section 5. In Section 6, we point out the consequences of our computations on Steinberg homology.

Acknowledgements. We would like to express our special thanks to Graham Ellis, who, by building a new feature into his HAP package in GAP upon our request, made it possible to remove the ambiguities in assembling our d_1 differential. We would like to heartily thank Bill Allombert (Pari/GP Development Headquarters), who helped us coding the GP script which formerly did run through all possibilities of assembling our d_1 differential, and still checks that the assembly is correct and produces the sanity check diagrams. We would like to warmly thank Simon King for having released his Mod- p Group Cohomology Package and answered our questions about it, and Matthias Köppe and especially Dmitrii Pasechnik for a lot of help on getting this package to run again in the contemporary version of SAGE. We are indebted to Peter Patzt for pointing us in Section 6 to the relevant theorems of Lee and Szczarba. Finally, we would like to thank Ethan Berkove for discussing the equivariant spectral sequence with us. We would like to acknowledge financial support by the ANR grant MELODIA (ANR-20-CE40-0013).

2. TORSION SUBCOMPLEX REDUCTION VIA DISCRETE MORSE THEORY

In order to reduce the ℓ -torsion subcomplex at a prime number ℓ (cf. Definition 1.2 above), our conditions for cancelling an n -cell τ against one of its boundary $(n-1)$ -cells σ , are the following ones, already established in previous work [20].

Condition 2.1. *As conditions for cancelling an n -cell τ against one of its boundary $(n-1)$ -cells σ , and hence for admitting an arrow from σ to τ into the discrete gradient vector field, we impose:*

- *No higher-dimensional cells of the ℓ -torsion subcomplex touch τ ,*
- *The interior of two cells connected by a path of the discrete gradient vector field do not contain two points which are on the same orbit under the group action,*
- *The inclusion of the stabilizer of τ into the stabilizer of σ induces an isomorphism on mod ℓ cohomology.*

Practical criteria for checking if an isomorphism on mod ℓ cohomology is induced are given in [20, Condition B’], based on control of ℓ -fusion.

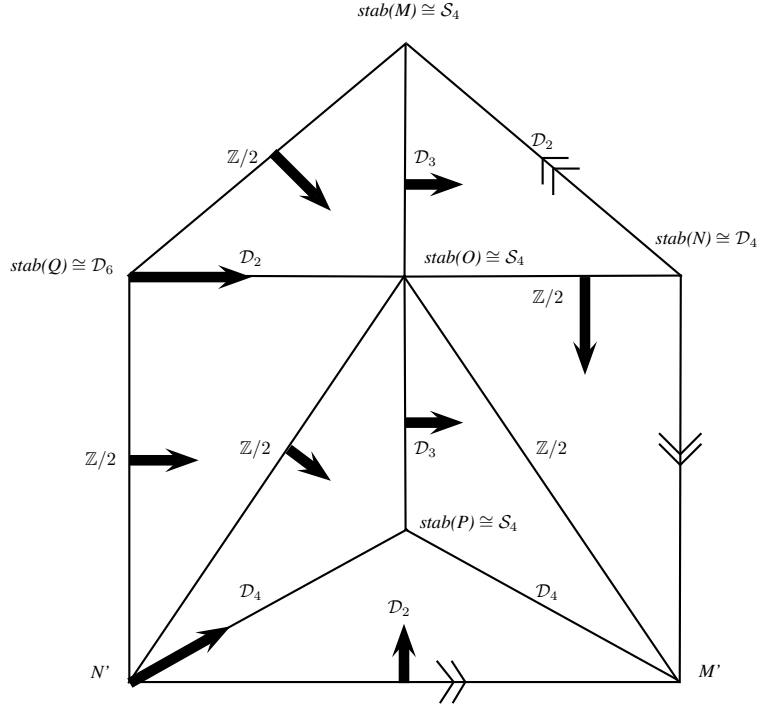
The mod ℓ equivariant cohomology is not affected by such a cancellation [20].

2.1. Construction of a discrete gradient vector field. In this section, we describe an algorithm constructing a discrete vector field for a discrete Morse function in the sense of Forman [13], with the extra property that ℓ -fusion is controlled along its arrows. We obtain it by inserting a fusion control condition into the *Discrete vector field on a regular CW-complex* algorithm of Ellis & Hegarty [12], see Algorithm 1 below. For this purpose, we need to recall the following definitions from the literature.

Definition 2.2. *A discrete vector field is said to be admissible if it contains no circuits and no chains that extend infinitely to the right. When the underlying CW-complex is finite, a discrete vector field is admissible if it contains no circuits.*

FIGURE 1. Example: The 2-torsion subcomplex for $SL_3(\mathbb{Z})$

On the 2-torsion subcomplex of the cell complex described by Soulé [24], obtained from the action of $SL_3(\mathbb{Z})$ on its symmetric space (diagram from previous work of one of the authors [20]), we draw here a discrete gradient vector field (in bold arrows).



Here, the three edges NM , NM' and $N'M'$ have to be identified as indicated by the double arrows. All of the seven triangles belong with their interior to the 2-torsion subcomplex, each with stabilizer $\mathbb{Z}/2$, except for the one which is marked to have stabilizer \mathcal{D}_2 . Along the discrete gradient vector field indicated by the simple arrows, we reduce this subcomplex to

$$\bullet \xrightarrow{\mathcal{S}_4} \bullet \xrightarrow{\mathbb{Z}/2} \bullet \xrightarrow{\mathcal{S}_4} \bullet \xrightarrow{\mathcal{D}_4} \bullet \xrightarrow{\mathcal{S}_4} \bullet$$

which is the geometric realization of Soulé's diagram of cell stabilizers. This yields the mod 2 Farrell–Tate cohomology as specified by Soulé [24].

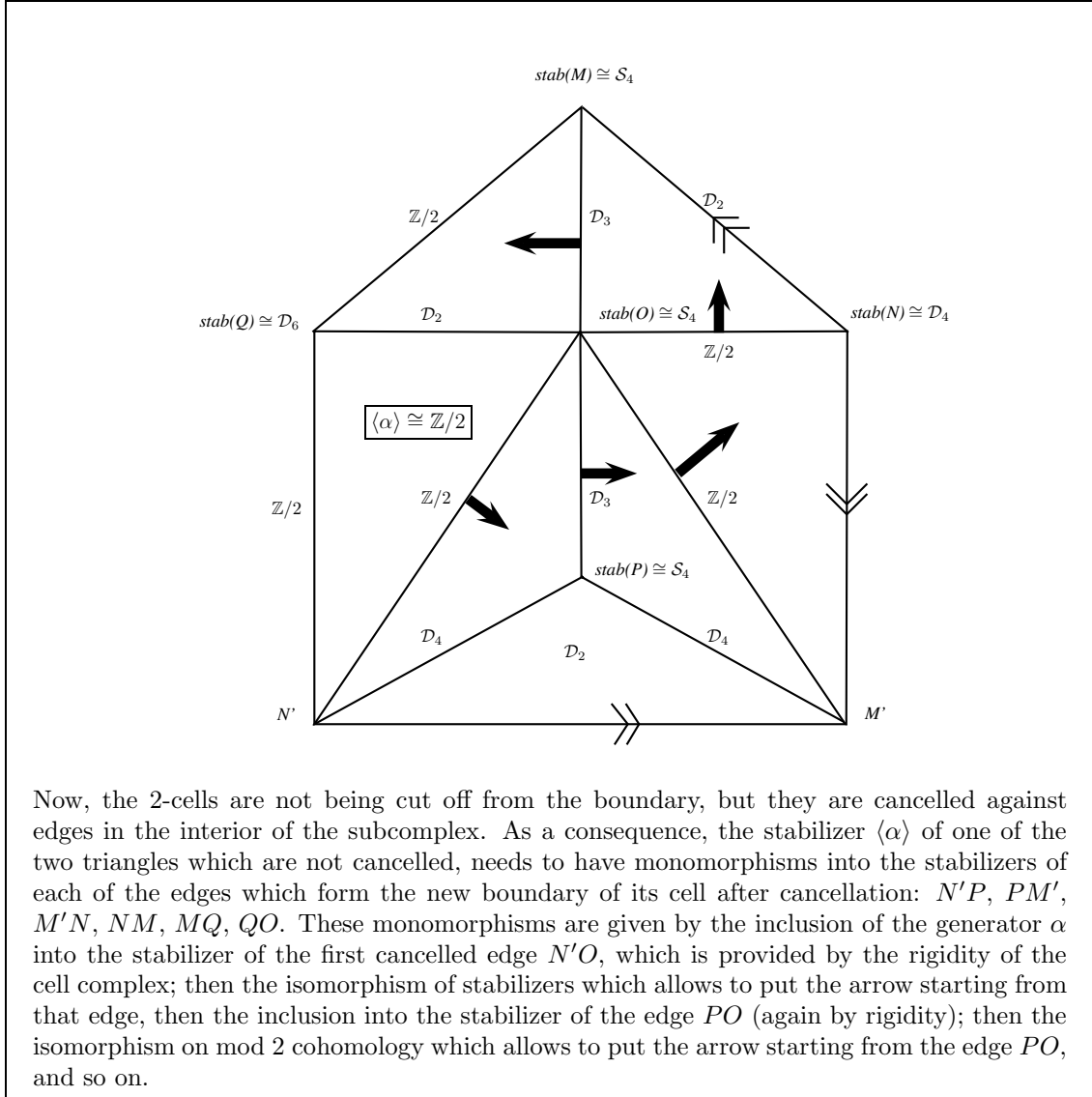
Definition 2.3. We say that an admissible discrete vector field is maximal if it is not possible to add an arrow while retaining admissibility. A cell in the CW-complex is said to be critical if it is not involved in any arrow.

In order to take the cell stabilizers into account, we need to equip the CW-complex with an extra structure, ensured by the terminology “simple complex of groups” introduced by Bridson and Haefliger [3, II.12.11 on page 375]:

Definition 2.4. Let X be a regular CW-complex. A simple complex of groups on X is a set $\{G_\sigma, \psi_{\tau\sigma}\}_{\sigma, \tau\sigma}$, where

- for each simplex $\sigma \in X$, we have a group G_σ ,
- for each cell τ in the boundary $\partial\sigma$ of a cell σ of X , we have an injective homomorphism $\psi_{\tau\sigma} : G_\sigma \rightarrow G_\tau$ such that if $\tau \in \partial\sigma$ and $\sigma \in \partial\rho$, then $\psi_{\tau\rho} = \psi_{\tau\sigma}\psi_{\sigma\rho}$.

FIGURE 2. We can also put an essentially different discrete gradient vector field on the 2-torsion subcomplex from Figure 1:



Now, the 2-cells are not being cut off from the boundary, but they are cancelled against edges in the interior of the subcomplex. As a consequence, the stabilizer $\langle \alpha \rangle$ of one of the two triangles which are not cancelled, needs to have monomorphisms into the stabilizers of each of the edges which form the new boundary of its cell after cancellation: $N'P$, PM' , $M'N$, NM , MQ , QO . These monomorphisms are given by the inclusion of the generator α into the stabilizer of the first cancelled edge $N'O$, which is provided by the rigidity of the cell complex; then the isomorphism of stabilizers which allows to put the arrow starting from that edge, then the inclusion into the stabilizer of the edge PO (again by rigidity); then the isomorphism on mod 2 cohomology which allows to put the arrow starting from the edge PO , and so on.

2.2. Critical cells and the equivariant spectral sequence. Once a maximal admissible discrete vector field has been constructed, we can reduce the torsion subcomplex by cancelling the two cells involved in an arrow against each other, such that only critical cells remain. For this purpose, we have to take care of what we shall call the boundary heritage.

Definition 2.5. *The boundary heritage of an n -cell which has some of its boundary cells cancelled by Morse reduction, consists for each cancelled boundary $(n-1)$ -cell σ of the non-cancelled boundary cells of the n -cell at the other end of the path leading to σ via the discrete gradient vector field.*

We can efficiently determine the boundary heritage by adapting Forman's construction of the Morse differential [13] to simple complexes of groups, as follows.

We take an $(n+1)$ -cell σ . For each n -cell $\tau \in \partial\sigma$, we can take the sum over all paths p (with signs coming from orientations of simplices) starting at τ , of the restriction maps $\mathrm{H}^\bullet(G_{\rho_p}) \rightarrow \mathrm{H}^\bullet(G_\sigma)$.

Algorithm 1 The *Discrete vector field on a regular CW-complex* algorithm of Ellis & Hegarty [12], with our fusion control condition inserted.

Input: A finite regular CW-complex Y carrying a simple complex of groups.

Output: A maximal admissible discrete vector field on Y .

procedure

Partially order the cells of Y in any fashion.

At any stage of the algorithm each cell will have precisely one of the following three states:

(i) *critical*, (ii) *potentially critical*, (iii) *non-critical*.

Initially deem all cells of Y to be potentially critical.

while there exists a potentially critical cell **do**

while there exists a pair of potentially critical cells s, t such that: $\dim(t) = \dim(s) + 1$; s lies in the boundary of t ; no other potentially critical cell of dimension $\dim(s)$ lies in the boundary of t , and Condition 2.1 is satisfied for the pair (s, t) ; **do**

 Choose such a pair (s, t) with s minimal in the given partial ordering.

 Add the arrow $s \rightarrow t$ and deem s and t to be non-critical.

end while

if there exists a potentially critical cell **then**

 Choose a minimal potentially critical cell and deem it to be critical.

end if

end while

end procedure

Here, G_{ρ_p} denotes the group at the end of the path p , and the group homomorphism is the composition of the isomorphism $G_\tau \cong G_{\rho_p}$ associated to the path p and the inclusion $G_\sigma \hookrightarrow G_\tau$.

Our above reflections culminate in the following theorem, which allows us to simplify the beginning of the equivariant spectral sequence.

Theorem 2.6. *Reducing an ℓ -torsion subcomplex consisting of finitely many orbits along a discrete gradient vector field constructed by Algorithm 1, and attaching the boundary heritage to replace lost boundary cells, induces an isomorphism on the E_2 page of the equivariant spectral sequence, and hence on equivariant mod ℓ cohomology.*

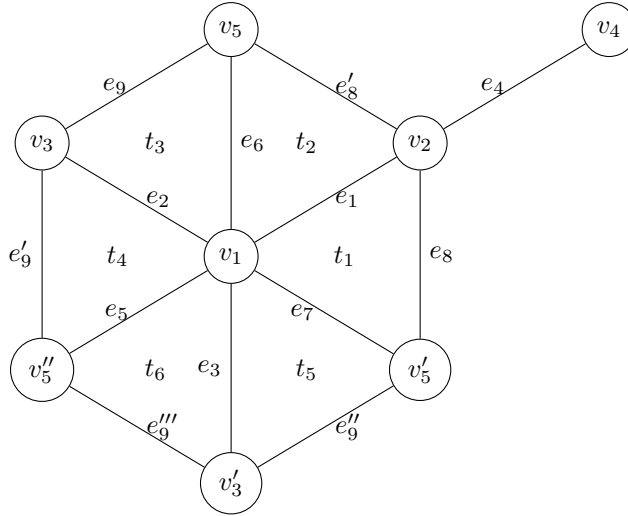
Proof. As we only have to deal with finitely many orbits modulo the group action, we can break down the reduction along the discrete vector field into finitely many steps of cancelling an n -cell against one of its boundary cells.

- For a path of n - and $(n-1)$ -cells through the discrete gradient vector field which starts at the boundary of the orbit space (see Figure 1), we can cancel one pair of cells after another without affecting the boundary of other cells, and each time, such a cancellation lowers the rank of the $d_1^{n-1,*}$ -differential as much as it the rank of the $E_1^{n-1,*}$ - and $E_1^{n,*}$ -terms of the equivariant spectral sequence. Hence the E_2 -page remains invariant, and thanks to our condition that no higher-dimensional cells of the ℓ -torsion subcomplex touch the concerned cells, no higher-degree differentials have targets on them, and hence the equivariant mod ℓ cohomology remains invariant as well.
- For a path through the discrete gradient vector field which is contained in the interior of the orbit space (see Figure 2), keeping track of the boundary heritage and attaching it to the neighbouring cells after each cancellation, is what makes sure that the cell structure is kept equivariant. Then we reach the claim via the same rank arguments as above.
- Fortunately, we cannot get into the situation of a circuit of arrows, because the discrete gradient vector field constructed by Algorithm 1 is admissible.

□

Remark 2.7. *We obtain an analogous algorithm for computing Bredon homology (useful if we want to continue the authors' Bredon homology computations [6] on larger cell complexes), namely*

FIGURE 3. A reduced 2-torsion subcomplex for $\mathrm{PSL}_4(\mathbb{Z})$. It is subject to the edge identifications $e_9 = e'_9 = e''_9 = e'''_9$ and $e_8 = e'_8$. The cell stabilizers are provided in Table 3.



by replacing the ℓ -fusion control condition in Condition 2.1 by the stronger condition that the two involved cell stabilizers are isomorphic.

2.3. Implementation and experimental evaluation. Theorem 2.6 allows us to simplify the beginning of the equivariant spectral sequence, using Algorithm 1. The authors’ implementation has been released in the HAP package of GAP [11], reducing the torsion subcomplexes along the discrete vector field [5]. On the 2-torsion subcomplex of $\mathrm{PSL}_4(\mathbb{Z})$, this brings down the runtime of the reduction procedure from a matter of days to a matter of seconds or at most minutes. That means, we could still do the 2-torsion calculation for $\mathrm{PSL}_4(\mathbb{Z})$ with the obsolete reduction procedure. But however, we choose this as our example for the rest of this paper, because for readers who want to tackle computations which are out of reach of the obsolete reduction procedure (for instance, on the 2-torsion subcomplexes of GL_3 over imaginary quadratic integers), our example computation can show how to overcome the difficulties which come next, once the reduction has been achieved.

3. SHOWCASE EXAMPLE: THE 2-TORSION SUBCOMPLEX FOR $\mathrm{PSL}_4(\mathbb{Z})$

The authors have run a machine computation, starting with a Voronoi cell complex with an action of $\mathrm{PSL}_4(\mathbb{Z})$, constructed by Dutour Sikiric [8], and available in the computer algebra system GAP [15] as part of the package HAP [11].

More precisely, $\mathrm{PSL}_4(\mathbb{Z})$ acts on a certain space of quadratic forms, and there is an equivariant retraction to Ash’s well-rounded retract [1]. On the latter co-compact space, a suitable form of Voronoi’s algorithm yields an explicit cell structure with cell stabilizers and computable quotient space, as described by Ellis, Dutour Sikiric and Schürmann in their paper on the integral homology of $\mathrm{PSL}_4(\mathbb{Z})$ [8].

In view of computing the cohomological 2-torsion, we want to extract the 2-torsion subcomplex from this Voronoi cell complex. As mentioned at the beginning of Section 2, we first need to make a subdivision to achieve a rigidity property and get the 2-torsion subcomplex to be a cell complex – this rigidity property is lacking on our Voronoi cell complex. We use “virtually simplicial subdivision” [6] for this purpose. Its implementation [5] also provides code to extract the 2-torsion subcomplex.

Next, we reduce the latter using the methods of Section 2, which are also implemented in the same sub-package of HAP [11]. The resulting reduced 2-torsion subcomplex is shown in Figure 3.

TABLE 3. Cell stabilizers in the reduced 2-torsion subcomplex for $\mathrm{PSL}_4(\mathbb{Z})$, and their cohomology rings.

| |
|---|
| <p>Denoting $\Gamma := \mathrm{PSL}_4(\mathbb{Z})$ and $\Gamma_\sigma := \{\gamma \in \Gamma : \gamma \cdot \sigma = \sigma\}$ the stabilizer of a cell σ, we observe the following stabilizers and their cohomology rings for the cells in Figure 3.</p> <p><u>Vertex stabilizers:</u></p> <p>$\Gamma_{v_1} \cong G_1$ with G_1 being the non-trivial group extension $1 \rightarrow \mathcal{A}_4 \times \mathcal{A}_4 \rightarrow G_1 \rightarrow \mathbb{Z}/2\mathbb{Z} \rightarrow 1$, $H^*(\Gamma_{v_1}; \mathbb{F}_2) \cong \mathbb{F}_2[c_{2,0}, c_{2,1}, b_{6,5}, b_{1,0}, b_{3,1}, b_{3,3}]/\langle b_{1,0} \cdot b_{3,1}, b_{1,0} \cdot b_{3,3}, b_{6,5} \cdot b_{1,0}, b_{6,5} \cdot b_{3,1} \cdot b_{3,3} + b_{6,5}^2 + c_{2,1}^3 \cdot b_{3,1}^2 + c_{2,0}^3 \cdot b_{3,3}^2 \rangle$.</p> <p>$\Gamma_{v_2} \cong \mathcal{S}_4$, $H^*(\Gamma_{v_2}; \mathbb{F}_2) \cong \mathbb{F}_2[\beta_1, \beta_2, \beta_3]/\langle \beta_1 \cdot \beta_3 \rangle$.</p> <p>$\Gamma_{v_3} \cong (\mathbb{Z}/2\mathbb{Z})^3$, $H^*(\Gamma_{v_3}; \mathbb{F}_2) \cong \mathbb{F}_2[\lambda_1, \mu_1, \nu_1]$.</p> <p>$\Gamma_{v_4} \cong \mathcal{S}_4$, $H^*(\Gamma_{v_4}; \mathbb{F}_2) \cong \mathbb{F}_2[\gamma_1, \gamma_2, \gamma_3]/\langle \gamma_1 \cdot \gamma_3 \rangle$.</p> <p>$\Gamma_{v_5} \cong G_2$ with G_2 obtained from the non-trivial extensions $1 \rightarrow G_0 \rightarrow G_2 \rightarrow \mathbb{Z}/2\mathbb{Z} \rightarrow 1$ and $1 \rightarrow (\mathbb{Z}/2\mathbb{Z})^4 \rightarrow G_0 \rightarrow \mathbb{Z}/3\mathbb{Z} \rightarrow 1$, $H^*(\Gamma_{v_5}; \mathbb{F}_2) \cong \mathbb{F}_2[\beta_{2,1}, \gamma_{2,0}, \gamma_{2,2}, \beta_{1,0}, \beta_{3,0}, \beta_{3,1}, \beta_{3,3}, \beta_{3,5}]/\langle \beta_{2,1} \cdot \beta_{1,0}, \beta_{1,0} \cdot \beta_{3,0}, \beta_{1,0} \cdot \beta_{3,1}, \beta_{1,0} \cdot \beta_{3,3}, \beta_{1,0} \cdot \beta_{3,5}, \beta_{2,1} \cdot \beta_{3,3} + \beta_{2,1} \cdot \beta_{3,1} + \gamma_{2,2} \cdot \beta_{3,3} + \gamma_{2,2} \cdot \beta_{3,1} + \gamma_{2,2} \cdot \beta_{3,0} + \gamma_{2,0} \cdot \beta_{3,3} + \gamma_{2,0} \cdot \beta_{3,1} + \gamma_{2,0} \cdot \beta_{3,0}, \beta_{2,1} \cdot \beta_{3,5} + \beta_{2,1} \cdot \beta_{3,1} + \gamma_{2,2} \cdot \beta_{3,5} + \gamma_{2,2} \cdot \beta_{3,3} + \gamma_{2,2} \cdot \beta_{3,1} + \gamma_{2,0} \cdot \beta_{3,5} + \gamma_{2,0} \cdot \beta_{3,3} + \gamma_{2,0} \cdot \beta_{3,0}, \beta_{3,1} \cdot \beta_{3,3} + \beta_{3,0} \cdot \beta_{3,1} + \beta_{3,0}^2 + \beta_{3,1}^2 + \beta_{2,1}^2 \cdot \gamma_{2,2} + \beta_{2,1}^2 \cdot \gamma_{2,0}, \beta_{3,1} \cdot \beta_{3,5} + \beta_{3,0} \cdot \beta_{3,3} + \beta_{3,0}^2 + \beta_{2,1}^3, \beta_{3,3}^2 + \beta_{3,0} \cdot \beta_{3,5} + \beta_{3,0}^2 + \beta_{2,1}^3 + \beta_{2,1}^2 \cdot \gamma_{2,2} \rangle$.</p> <p><u>Edge stabilizers:</u></p> <p>$\Gamma_{e_1} \cong \mathbb{Z}/4\mathbb{Z}$, $H^*(\Gamma_{e_1}; \mathbb{F}_2) \cong \mathbb{F}_2[c_1, c_2]/\langle c_1^2 \rangle$.</p> <p>$\Gamma_{e_2} \cong (\mathbb{Z}/2\mathbb{Z})^2$, $H^*(\Gamma_{e_2}; \mathbb{F}_2) \cong \mathbb{F}_2[x_1, y_1]$.</p> <p>$\Gamma_{e_3} \cong (\mathbb{Z}/2\mathbb{Z})^2$, $H^*(\Gamma_{e_3}; \mathbb{F}_2) \cong \mathbb{F}_2[b_1, v_1]$.</p> <p>$\Gamma_{e_4} \cong \mathcal{D}_8$, $H^*(\Gamma_{e_4}; \mathbb{F}_2) \cong \mathbb{F}_2[r_1, t_1, t_2]/\langle t_1^2 + r_1 \cdot t_1 \rangle$.</p> <p>$\Gamma_{e_5} \cong \mathbb{Z}/2\mathbb{Z}$, $H^*(\Gamma_{e_5}; \mathbb{F}_2) \cong \mathbb{F}_2[b_1]$.</p> <p>$\Gamma_{e_6} \cong \mathcal{D}_8$, $H^*(\Gamma_{e_6}; \mathbb{F}_2) \cong \mathbb{F}_2[a_1, s_1, s_2]/\langle a_1 \cdot s_1 \rangle$.</p> <p>$\Gamma_{e_7} \cong \mathcal{D}_8$, $H^*(\Gamma_{e_7}; \mathbb{F}_2) \cong \mathbb{F}_2[a'_1, w_1, w_2]/\langle a'_1 \cdot w_1 \rangle$.</p> <p>$\Gamma_{e_9} \cong (\mathbb{Z}/2\mathbb{Z})^3$, $H^*(\Gamma_{e_9}; \mathbb{F}_2) \cong \mathbb{F}_2[x'_1, y'_1, z_1]$.</p> <p><u>Triangle stabilizers:</u></p> <p>$\Gamma_{t_1} = \Gamma_{t_2} \cong \mathbb{Z}/2\mathbb{Z}$, $H^*(\Gamma_{t_1}; \mathbb{F}_2) \cong \mathbb{F}_2[\widehat{a}_1]$.</p> <p>$\Gamma_{t_3} \cong (\mathbb{Z}/2\mathbb{Z})^2$, $H^*(\Gamma_{t_3}; \mathbb{F}_2) \cong \mathbb{F}_2[\widehat{x}_1, \widehat{y}_1]$.</p> <p>$\Gamma_{t_4} = \Gamma_{t_6} \cong \mathbb{Z}/2\mathbb{Z}$, $H^*(\Gamma_{t_4}; \mathbb{F}_2) \cong \mathbb{F}_2[b_1]$.</p> <p>$\Gamma_{t_5} \cong (\mathbb{Z}/2\mathbb{Z})^2$, $H^*(\Gamma_{t_5}; \mathbb{F}_2) \cong \mathbb{F}_2[\widehat{u}_1, \widehat{v}_1]$.</p> |
|---|

3.1. The cell stabilizers and their cohomology rings. With a GAP script [7], we generate a SAGE [23] script containing matrix representations of the cell stabilizer maps from that reduced 2-torsion-subcomplex, with which the individual ring homomorphisms induced between the cell stabilizers' cohomology rings can be computed with King's package [17] in SAGE version 9.6beta4. Its output is provided in the supplementary materials of this paper [7], and yields the cohomology ring presentations in Table 3.

Remark 3.1. *Note that we merge the 2-cells t_1 and t_2 along their common edge e_8 (these three cells have isomorphic stabilizers). But we may not merge the 2-cells t_4 and t_6 along their common edge e_5 : Also these three cells have isomorphic stabilizers, but there are two copies of the edge e_9 adjacent, and two further copies of e_9 non-adjacent to t_4 and t_6 . This forbidden merge would prevent the diagram in Figure 5 from commuting. However, in order to simplify the diagram in Figure 4, we think of t_4 and t_6 being virtually merged just when chasing through that diagram.*

Then we assemble these cohomology ring maps, using the new HAP functions written for this purpose by Ellis, and available in the current version of HAP [11], with which commutative diagrams of finite groups can be used to induce commutative diagrams on mod ℓ (especially at $\ell = 2$) cohomology of those groups, keeping track of the cup product structure. Before, keeping track of the cup product structure in HAP was possible only when the finite groups were “prime power” / “ ℓ -groups”: All their elements had to be of order a power of the same prime. This restriction has been lifted with Ellis' new functions. We enter all those of the commutative diagrams of the 2-torsion subcomplex of $\mathrm{PSL}_4(\mathbb{Z})$ which have to commute simultaneously. As this allows it to read out in HAP what happens in degrees 1 to 4 of the cup product structure [7], we are able to assemble the d_1 differential from our information about the individual cohomology ring maps obtained with King's package [17] - see our collection of induced maps (19 handwritten pages) on the generators of the stabilizer's cohomology rings, which make all the 16 diagrams (on

14 handwritten pages) commute [7]. We then use a Pari/GP [19] script, developed with the help of Allombert, to check back the equation $d_1^{1,*} \circ d_1^{0,*} \equiv 0 \pmod{2}$ which results from the commutativity of the diagrams. This Pari/GP script [7] also outputs these diagrams (Figures 4, 5 and 6) and the d_1 differential (Table 4). The assembled d_1 differential (Table 4) is then manually coded into a SAGE script [7] which computes from it the E_2 page in a range of feasible degrees, as shown in Table 5.

4. THE d_1 DIFFERENTIAL FOR $\mathrm{PSL}_4(\mathbb{Z})$

The bulk of the six years which this paper took to mature, went into establishing the d_1 differential (Table 4). King's SAGE package [17] allows to induce the individual cohomology ring maps from the cell stabilizer maps, but the relations between them are getting lost as the ring presentations are obtained by calls to the SINGULAR computer algebra system. Various ideas on how to ensure coherence on the choices of ring presentations were explored, until finally Ellis did extend the functionality of his GAP package HAP [11], such that we can trace precisely what happens with the cohomology classes of degrees 1, 2 and 3 (see the 19 handwritten pages in [7]). This removes all ambiguities.

4.1. Sanity check: Commutative diagrams verified by the d_1 differential. The vanishing of the concatenation $d_1^{1,q} \circ d_1^{0,q} \equiv 0 \pmod{2}$ is ensured by the commutative diagrams of ring generators of the cohomology rings of the finite cell stabilizer groups, displayed in Figures 4, 5 and 6.

FIGURE 4. Commutative diagram of mappings of the cohomology ring generators of the 1st vertex stabilizer.

$$\begin{array}{ccccc}
 \begin{pmatrix} 0 \\ \tilde{a}_1^2 \\ 0 \\ 0 \\ 0 \\ 0 \end{pmatrix} & \xleftarrow{t_1 \cup t_2} & \begin{pmatrix} w_2 \\ w_2 + a_1'^2 + w_1^2 \\ a_1'^4 \cdot w_2 \\ w_1 \\ a_1' \cdot w_2 \\ a_1' \cdot w_2 \end{pmatrix} & \xrightarrow{t_5} & \begin{pmatrix} \tilde{u}_1^2 + \tilde{v}_1 \cdot \tilde{u}_1 + \tilde{v}_1^2 \\ \tilde{v}_1 \cdot \tilde{u}_1 + \tilde{v}_1^2 \\ 0 \\ \tilde{u}_1 \\ 0 \\ 0 \end{pmatrix} \\
 \uparrow t_1 \cup t_2 & & \uparrow e_7 & & \uparrow t_5 \\
 \begin{pmatrix} s_1^2 + s_2 \\ a_1^2 \\ a_1^4 \cdot s_2 \\ s_1 \\ a_1 \cdot s_2 \\ 0 \end{pmatrix} & \xleftarrow{e_6} & \begin{pmatrix} c_{2,0} \\ c_{2,1} \\ b_{6,5} \\ b_{1,0} \\ b_{3,1} \\ b_{3,3} \end{pmatrix} & \xrightarrow{e_3} & \begin{pmatrix} b_1^2 + v_1 \cdot b_1 + v_1^2 \\ v_1 \cdot b_1 + v_1^2 \\ 0 \\ b_1 \\ 0 \\ 0 \end{pmatrix} \\
 \downarrow t_3 & & \downarrow e_2 & & \downarrow t_4 \cup t_6 \\
 \begin{pmatrix} \tilde{x}_1^2 + \tilde{y}_1 \cdot \tilde{x}_1 + \tilde{y}_1^2 \\ 0 \\ 0 \\ \tilde{x}_1 + \tilde{y}_1 \\ 0 \\ 0 \end{pmatrix} & \xleftarrow{t_3} & \begin{pmatrix} x_1^2 + y_1 \cdot x_1 + y_1^2 \\ 0 \\ 0 \\ x_1 + y_1 \\ 0 \\ 0 \end{pmatrix} & \xrightarrow{t_4 \cup t_6} & \begin{pmatrix} \tilde{b}_1^2 \\ 0 \\ 0 \\ \tilde{b}_1 \\ 0 \\ 0 \end{pmatrix}
 \end{array}$$

TABLE 4. The d_1 differential on the generators of the cohomology rings of the cell stabilizers, referring to the ring presentations given in Table 3.

| $d_1^{0,*}$ | $v_1 : c_{2,0}, c_{2,1}, b_{6,5}, b_{1,0}, b_{3,1}, b_{3,3}$ | $v_2 : \beta_1, \beta_2, \beta_3$ | $v_3 : \lambda_1, \mu_1, \nu_1$ | $v_4 : \gamma_1, \gamma_2, \gamma_3$ |
|-------------|--|---|---------------------------------|---|
| $e_1 :$ | $0, c_2, 0, c_1, 0, c_1 \cdot c_2$ | $c_1, c_2, c_1 \cdot c_2$ | $0, 0, 0$ | $0, 0, 0$ |
| $e_2 :$ | $x_1^2 + y_1 \cdot x_1 + y_1^2, 0, 0, x_1 + y_1, 0, 0$ | $0, 0, 0$ | x_1, x_1, y_1 | $0, 0, 0$ |
| $e_3 :$ | $b_1^2 + v_1 \cdot b_1 + v_1^2, v_1 \cdot b_1 + v_1^2, 0, b_1, 0, 0$ | $0, 0, 0$ | $b_1, v_1, 0$ | $0, 0, 0$ |
| $e_4 :$ | $0, 0, 0, 0, 0, 0$ | $t_1 + t_1, t_1^2 + t_2, t_2 \cdot t_1$ | $0, 0, 0$ | $t_1, t_2, t_2 \cdot t_1 + t_2 \cdot t_1$ |
| $e_5 :$ | $\tilde{b}_1^2, 0, 0, \tilde{b}_1, 0, 0$ | $0, 0, 0$ | $0, 0, 0$ | $0, 0, 0$ |
| $e_6 :$ | $s_1^2 + s_2, a_1^2, a_1^4 \cdot s_2, s_1, a_1 \cdot s_2, 0$ | $0, 0, 0$ | $0, 0, 0$ | $0, 0, 0$ |
| $e_7 :$ | $w_2, w_2 + a_1^2 + w_1^2, a_1^4 \cdot w_2, w_1, a_1 \cdot w_2, a_1 \cdot w_2$ | $0, 0, 0$ | $0, 0, 0$ | $0, 0, 0$ |
| $e_9 :$ | $0, 0, 0, 0, 0, 0$ | $0, 0, 0$ | $y_1', z_1, z_1 + x_1'$ | $0, 0, 0$ |

| $d_1^{0,*}$ | $v_5 : \beta_{2,1}, \gamma_{2,0}, \gamma_{2,2}, \beta_{1,0}, \beta_{3,0}, \beta_{3,1}, \beta_{3,3}, \beta_{3,5}$ |
|-------------|--|
| $e_1 :$ | $0, 0, 0, 0, 0, 0, 0, 0$ |
| $e_2 :$ | $0, 0, 0, 0, 0, 0, 0, 0$ |
| $e_3 :$ | $0, 0, 0, 0, 0, 0, 0, 0$ |
| $e_4 :$ | $0, 0, 0, 0, 0, 0, 0, 0$ |
| $e_5 :$ | $\tilde{b}_1^2, 0, 0, 0, \tilde{b}_1^3, \tilde{b}_1^3, 0, 0$ |
| $e_6 :$ | $s_1^2, s_2, s_2 + a_1^2, a_1, s_1^3 + s_2 \cdot s_1, s_1^3 + s_2 \cdot s_1, 0, s_2 \cdot s_1$ |
| $e_7 :$ | $w_1^2, w_2 + w_1^2, a_1^2, a_1^4 \cdot w_1 \cdot w_2, w_1^3, 0, w_1 \cdot w_2 + w_1^3$ |
| $e_9 :$ | $\begin{pmatrix} y_1'^2 + (z_1 + x_1') \cdot y_1' + x_1' \cdot z_1 + x_1'^2, \\ z_1 \cdot y_1' + x_1' \cdot z_1, \\ z_1^2 + x_1' \cdot z_1, \\ 0, \\ y_1'^3 + x_1' \cdot y_1'^2 + z_1^2 \cdot y_1' + x_1'^2 \cdot z_1 + x_1'^3, \\ y_1'^3 + (z_1 + x_1') \cdot y_1'^2 + x_1'^2 \cdot z_1 + x_1'^3, \\ 0, \\ z_1 \cdot y_1'^2 + z_1^2 \cdot y_1' + x_1' \cdot z_1^2 + x_1'^2 \cdot z_1 \end{pmatrix}$ |

| $d_1^{1,*}$ | $e_1 :$ c_1, c_2 | $e_2 :$ x_1, y_1 | $e_3 :$ b_1, v_1 | $e_4 :$ r_1, t_1, t_2 | $e_5 :$ \tilde{b}_1 | $e_6 :$ a_1, s_1, s_2 | $e_7 :$ a_1', w_1, w_2 | $e_9 :$ x_1', y_1', z_1 |
|------------------|-----------------------|----------------------------|----------------------------|----------------------------|--------------------------|---|---|---|
| $t_1 \cup t_2 :$ | $0, 0$ | $0, 0$ | $0, 0$ | $0, 0, 0$ | 0 | $\tilde{a}_1, 0, 0$ | $\tilde{a}_1, 0, 0$ | $0, 0, 0$ |
| $t_3 :$ | $0, 0$ | \tilde{x}_1, \tilde{y}_1 | $0, 0$ | $0, 0, 0$ | 0 | $0, \tilde{x}_1 + \tilde{y}_1, \tilde{y}_1 \cdot \tilde{x}_1$ | $0, 0, 0$ | $\tilde{x}_1 + \tilde{y}_1, \tilde{x}_1, \tilde{x}_1$ |
| $t_4 :$ | $0, 0$ | $0, \tilde{b}_1$ | $0, 0$ | $0, 0, 0$ | \tilde{b}_1 | $0, 0, 0$ | $0, 0, 0$ | $\tilde{b}_1, 0, 0$ |
| $t_5 :$ | $0, 0$ | $0, 0$ | \tilde{u}_1, \tilde{v}_1 | $0, 0, 0$ | 0 | $0, 0, 0$ | $0, \tilde{u}_1, \tilde{u}_1^2 + \tilde{v}_1 \cdot \tilde{u}_1 + \tilde{v}_1^2$ | $\tilde{v}_1, \tilde{u}_1, \tilde{v}_1$ |
| $t_6 :$ | $0, 0$ | $0, 0$ | $\tilde{b}_1, 0$ | $0, 0, 0$ | \tilde{b}_1 | $0, 0, 0$ | $0, 0, 0$ | $0, \tilde{b}_1, 0$ |

FIGURE 5. Commutative diagram of mappings of the cohomology ring generators of the 3rd vertex stabilizer.

$$\begin{array}{ccccc}
\begin{pmatrix} \tilde{u}_1 \\ \tilde{v}_1 \\ 0 \end{pmatrix} & \xleftarrow{t_5} & \begin{pmatrix} b_1 \\ v_1 \\ 0 \end{pmatrix} & \xrightarrow{t_6} & \begin{pmatrix} \tilde{b}_1 \\ 0 \\ 0 \end{pmatrix} \\
\uparrow t_5 & & \uparrow e_3 & & \uparrow t_6 \\
\begin{pmatrix} y_1' \\ z_1 \\ z_1 + x_1' \end{pmatrix} & \xleftarrow{e_9} & \begin{pmatrix} \lambda_1 \\ \mu_1 \\ \nu_1 \end{pmatrix} & \xrightarrow{e_9} & \begin{pmatrix} y_1' \\ z_1 \\ z_1 + x_1' \end{pmatrix} \\
\downarrow t_3 & & \downarrow e_2 & & \downarrow t_4 \\
\begin{pmatrix} \tilde{x}_1 \\ \tilde{x}_1 \\ \tilde{y}_1 \end{pmatrix} & \xleftarrow{t_3} & \begin{pmatrix} x_1 \\ x_1 \\ y_1 \end{pmatrix} & \xrightarrow{t_4} & \begin{pmatrix} 0 \\ 0 \\ \tilde{b}_1 \end{pmatrix}
\end{array}$$

FIGURE 6. Commutative diagram of mappings of the cohomology ring generators of the 5th vertex stabilizer.

$$\begin{array}{ccccc}
 & & \begin{pmatrix} \widetilde{u}_1^2 \\ \widetilde{v}_1^2 + \widetilde{u}_1 \cdot \widetilde{v}_1 \\ 0 \\ 0 \\ \widetilde{u}_1^3 + \widetilde{u}_1^2 \cdot \widetilde{v}_1 + \widetilde{u}_1 \cdot \widetilde{v}_1^2 \\ \widetilde{u}_1^3 \\ 0 \\ \widetilde{u}_1^2 \cdot \widetilde{v}_1 + \widetilde{u}_1 \cdot \widetilde{v}_1^2 \end{pmatrix} & & \\
 & \nearrow t_5 & & \nwarrow t_5 & \\
 \begin{pmatrix} x_1'^2 + x_1' \cdot y_1' + x_1' \cdot z_1 + y_1'^2 + y_1' \cdot z_1 \\ x_1' \cdot z_1 + y_1' \cdot z_1 \\ x_1' \cdot z_1 + z_1^2 \\ 0 \\ x_1'^3 + x_1'^2 \cdot z_1 + y_1'^3 + y_1' \cdot z_1^2 + x_1' \cdot y_1'^2 \\ x_1' \cdot y_1'^2 + y_1'^3 + y_1'^2 \cdot z_1 + x_1'^3 + x_1'^2 \cdot z_1 \\ 0 \\ x_1'^2 \cdot z_1 + x_1' \cdot z_1^2 + y_1'^2 \cdot z_1 + y_1' \cdot z_1^2 \end{pmatrix} & & & & \begin{pmatrix} w_1^2 \\ w_1^2 + w_2 \\ a_1'^2 \\ a_1' \\ w_2 \cdot w_1 \\ w_1^3 \\ 0 \\ w_1^3 + w_2 \cdot w_1 \end{pmatrix} \\
 & \nearrow e_9 & & \nearrow e_7 & \\
 & & \begin{pmatrix} \beta_{2,1} \\ \gamma_{2,0} \\ \gamma_{2,2} \\ \beta_{1,0} \\ \beta_{3,0} \\ \beta_{3,1} \\ \beta_{3,3} \\ \beta_{3,5} \end{pmatrix} & & \\
 & \downarrow t_3 & & & \downarrow t_1 \cup t_2 \\
 \begin{pmatrix} \widetilde{x}_1^2 + \widetilde{y}_1^2 \\ \widetilde{x}_1 \cdot \widetilde{y}_1 \\ \widetilde{x}_1 \cdot \widetilde{y}_1 \\ 0 \\ \widetilde{x}_1^3 + \widetilde{y}_1^3 \\ \widetilde{x}_1^3 + \widetilde{y}_1^3 \\ 0 \\ \widetilde{x}_1^2 \cdot \widetilde{y}_1 + \widetilde{x}_1 \cdot \widetilde{y}_1^2 \end{pmatrix} & & & & \begin{pmatrix} 0 \\ 0 \\ \widetilde{a}_1^2 \\ \widetilde{a}_1 \\ 0 \\ 0 \\ 0 \\ 0 \end{pmatrix} \\
 & \nearrow t_3 & & \nearrow t_1 \cup t_2 & \\
 & & \begin{pmatrix} s_1^2 \\ s_2 \\ s_2 + a_1^2 \\ a_1 \\ s_1^3 + s_2 \cdot s_1 \\ s_1^3 + s_2 \cdot s_1 \\ 0 \\ s_2 \cdot s_1 \end{pmatrix} & &
 \end{array}$$

5. SPECTRAL SEQUENCE EVALUATION AND MOD 2 FARRELL–TATE COHOMOLOGY OF $\mathrm{PSL}_4(\mathbb{Z})$

From the E_2 -page shown in Table 5, we see that the d_2 differential must be trivial, and hence the spectral sequence degenerates at that stage.

TABLE 5. The E_2 -page of our equivariant spectral sequence.

In all observed degrees $q \geq 2$, the differential $d_1^{0,q}$ is surjective, and hence at $q \geq 2$, the E_2 -page is concentrated in the single column $p = 0$. In that column, we record the dimensions over \mathbb{F}_2 for $E_2^{0,q}$ for $7 \leq q \leq 42$ in Table 1. In all degrees $q \geq 0$, the E_2 -page is concentrated in three columns, which we display here for $q \leq 6$:

| | | | |
|---------|---------------------|----------------|----------------|
| $q = 6$ | \mathbb{F}_2^{27} | 0 | 0 |
| $q = 5$ | \mathbb{F}_2^{17} | 0 | 0 |
| $q = 4$ | \mathbb{F}_2^7 | 0 | 0 |
| $q = 3$ | \mathbb{F}_2^7 | 0 | 0 |
| $q = 2$ | \mathbb{F}_2^3 | 0 | 0 |
| $q = 1$ | 0 | \mathbb{F}_2 | 0 |
| $q = 0$ | \mathbb{F}_2 | 0 | \mathbb{F}_2 |
| | $p = 0$ | $p = 1$ | $p = 2$ |

From the E_2 -page calculated in Table 5, we deduce our results on the mod-2 Farrell–Tate cohomology of $\mathrm{PSL}_4(\mathbb{Z})$, presented in Theorem 1.1 in the Introduction.

6. IMPLICATIONS ON STEINBERG HOMOLOGY

In the long exact sequence connecting Farrell–Tate cohomology, group cohomology and Steinberg homology (cf. the chapter on Farrell–Tate cohomology in Brown’s book [4]), we insert our results on Farrell–Tate cohomology $\widehat{H}^* := \widehat{H}^*(\mathrm{PSL}_4(\mathbb{Z}); \mathbb{F}_2)$, the results of Dutour, Ellis and Schürmann [8] on group cohomology $H^* := H^*(\mathrm{PSL}_4(\mathbb{Z}); \mathbb{F}_2)$, and on Steinberg homology \widetilde{H}_* the result $\widetilde{H}_0 = 0$ of Lee and Szczarba [18, theorems 1.3 and 4.1, lemma 4.2]. Then we can speculate on the Steinberg homology in the other degrees (the numbers inserted here with a question mark assume the case of trivial connection maps in the long exact sequence, and the reader can easily adjust them to cases of non-trivial connection map ranks). The top line of this long exact sequence demonstrates the compatibility of our results with $\widetilde{H}_0 = 0$ and the results of Dutour, Ellis and Schürmann.

- [20] Alexander D. Rahm, *An introduction to torsion subcomplex reduction*, Advanced Studies: Euro-Tbilisi Mathematical Journal **9** (2021), pages 105-126, Special issue on Cohomology, Geometry, Explicit Number Theory.
- [21] ———, *Accessing the cohomology of discrete groups above their virtual cohomological dimension*, J. Algebra **404** (2014), 152–175. MR3177890
- [22] ———, *The homological torsion of PSL_2 of the imaginary quadratic integers*, Trans. Amer. Math. Soc. **365** (2013), no. 3, 1603–1635, DOI 10.1090/S0002-9947-2012-05690-X. MR3003276
- [23] The Sage Developers, *Sagemath, the Sage Mathematics Software System (Version 9.6beta4)*, 2022. doi.org/10.5281/zenodo.820864 <https://www.sagemath.org>.
- [24] Christophe Soulé, *The cohomology of $\mathrm{SL}_3(\mathbf{Z})$* , Topology **17** (1978), no. 1, 1–22.
- [25] Naya Yerolemou and Vidit Nanda, *Morse theory for complexes of groups*, J. Pure Appl. Algebra **228** (2024), no. 6, Paper No. 107606, 31, DOI 10.1016/j.jpaa.2024.107606.

¹FACULTY OF MATHEMATICS AND COMPUTER SCIENCE, UNIVERSITY OF SCIENCE, HO CHI MINH CITY, VIETNAM

²VIETNAM NATIONAL UNIVERSITY, HO CHI MINH CITY, VIETNAM

³LABORATOIRE DE MATHÉMATIQUES GAATI, UNIVERSITÉ DE LA POLYNÉSIE FRANÇAISE, BP 6570, 98702 FAA'A, FRENCH POLYNESIA, ALEXANDER.RAHM@UPF.PF , ORCID: 0000-0002-5534-2716, [HTTPS://GAATI.ORG/RAHM](https://gaati.org/rahm)

⁴MATTHIAS WENDT, FACHGRUPPE MATHEMATIK/INFORMATIK, BERGISCHE UNIVERSITÄT WUPPERTAL, GAUSSSTRASSE 20, 42119 WUPPERTAL, GERMANY